RSC Advances

PAPER

View Article Online
View Journal | View Issue

Cite this: *RSC Adv.*, 2017, **7**, 9309

Light-induced synthesis of triazine N-oxide-based cross-linked polymers for effective photocatalytic degradation of methyl orange†

Yangxue Li,*[a] Wei Zhang,[b] Jian Wang,[d] Haojie Lu,[a] Yu Liu,[d] Zhi Liu[c] and Zhigang Xie[b]

Received 20th October 2016
Accepted 19th January 2017

DOI: 10.1039/c6ra25532a

rsc.li/rsc-advances

The scarcity of clean water and increasing environmental pollution are critical issues owing to the rapid development of industrialisation, population growth and long-term droughts. Research and development of robust photocatalysts is very important to treat recalcitrant organic dye wastewater. Porous organic polymers are favored as a new type of photocatalyst owing to their high specific surface area and porosity. Here, two novel 2D cross-linked polymers LCP-1 (Light-induced Cross-linked Polymer 1) and LCP-2 (Light-induced Cross-linked Polymer 2) were synthesized through light-induced click cross-coupling reaction. Starting from LCP-1 and LCP-2 as supports, the polymeric aromatic N-oxides (LCPO-1 and LCPO-2) were prepared through the reaction of the nitrogen-containing aromatic heterocycle and peroxyacetic acid at 333 K, respectively. The structure and morphology were studied by IR, solid-state ^{13}C NMR, TEM and SEM. The polymeric aromatic N-oxides (LCPO-1 and LCPO-2) as organic metal-free photocatalysts showed great potential in the photodegradation of methyl orange (MO) in solution. The turn over number (TON) and the turn over frequency (TOF) of the catalysts varied and depended on the structures. For LCPO-1, the calculated TOF of the catalyst for the three cycles were determined, which were 4.83×10^{16}, 2.50×10^{16} and 2.00×10^{16} molecules per g per s, while for LCPO-2 were 4.00×10^{16}, 2.40×10^{16} and 1.67×10^{16} molecules per g per s, respectively.

Introduction

Organic dyes are widely used in food, medicine, printing and dyeing, cosmetics and so on, with more than 1×10^5 types in commercial use.[1] According to statistics, Chinese dye production of 1.5×10^5 tons is ranked at the forefront of world dye production of 8×10^5 to 9×10^5 tons per year.[2] With the extensive use of various dyes, approximately 10–15% of them will finally end up in discharged effluents.[3,4] Most of these dyes are extremely stable, so it is difficult for them to be degraded naturally, increasing the color of polluted water, influencing the amount of incident light, and then affecting the normal life activities of aquatic animals and plants, causing eutrophication in stagnant water bodies.[5–7] More serious is that dyes with carcinogenic and mutagenic effects are discharged into the environment, posing a great threat to the health of human beings and other living creatures.[8] Thus, the removal of these organic contaminants has become one of the most important environmental issues worldwide.

As solar energy, radiant light and heat from the sun are considered to be the most abundant clean energy sources available, utilizing and conversion of solar energy is the most promising way to solve the energy crisis and environmental pollution in the world.[9] An effective tool to overcome this obstacle is to develop novel photocatalytic materials that convert light energy into chemical energy and promote the decomposition and synthesis of organic compounds.[10–13] Specifically, ever since the discovery of water photolysis on a TiO_2 electrode by Fujishima, inorganic materials, metal oxide or sulfide semiconductor materials, such as TiO_2, ZnO, CdS, SnO_2 and WO_3, have proved to be efficient in depollution of water from toxic chemicals as photocatalysts.[14–19] However, there are several key problems that influence their large-scale industrial practical application including: (1) the light response range is narrow, the large band gap (3.2 eV) of TiO_2 largely limits its photocatalytic activity in the UV light region, which is less than 5% of the solar spectrum to the ground; (2) the quantum efficiency is low, not more than 28% at most; (3) retrievability and regeneration are difficult. Therefore, developing photocatalysts with high efficiency, good stability and

[a]College of Environment and Resources, Jilin University, Changchun 130026, P. R. China. E-mail: yangxueli@jlu.edu.cn

[b]State Key Laboratory of Polymer Physics and Chemistry, Changchun Institute of Applied Chemistry, Chinese Academy of Sciences, 5625 Renmin Street, Changchun 130022, P. R. China

[c]Jilin Province ShunFood Technology Services Limited Liability Company, Changchun 13000, P. R. China

[d]State Key Laboratory of Theoretical and Computational Chemistry, Institute of Theoretical Chemistry, Jilin University, Changchun 130023, P. R. China

† Electronic supplementary information (ESI) available: Characterization figure and supporting figures. See DOI: 10.1039/c6ra25532a

good reusability simultaneously has become one of the noble missions of material science.

On the other hand, cross-linked polymers represent a new class of robust and porous materials composed of organic molecules connected by covalent bonds, and with their low density and stable structure have attracted widespread attention.[20–34] Unlike inorganic materials, cross-linked polymers, with higher reactivity and quantum yield owing to their high specific surface area and porosity, are favored as a new type of photocatalyst.[35–40] More importantly, the properties of cross-linked polymers can be facilely tuned and modified by modular synthesis and selection of monomers. Synthesis of cross-linked polymers usually requires harsh conditions and the use of catalysts.[41,42] Developing simple, mild, environmentally friendly and efficient reactions is still a big challenge in this field. Light as a common energy donor has been applied in driving many chemical reactions.[43–48] Herein, two cross-linked polymers LCP-1 (Light-induced Cross-linked Polymer 1) and LCP-2 (Light-induced Cross-linked Polymer 2) were prepared through light irradiation; then, polymeric aromatic N-oxides (LCPO-1 and LCPO-2) were afforded by introducing N–O bonds on the polymers (Scheme 1). The changed polarity, hydrophilicity and electronic structure improving the harvesting of solar light and the photocatalytic ability. As a result, the polymeric aromatic N-oxides (LCPO-1 and LCPO-2) could be used as novel organic heterogeneous photocatalysts for degradation of pollutants in wastewater.

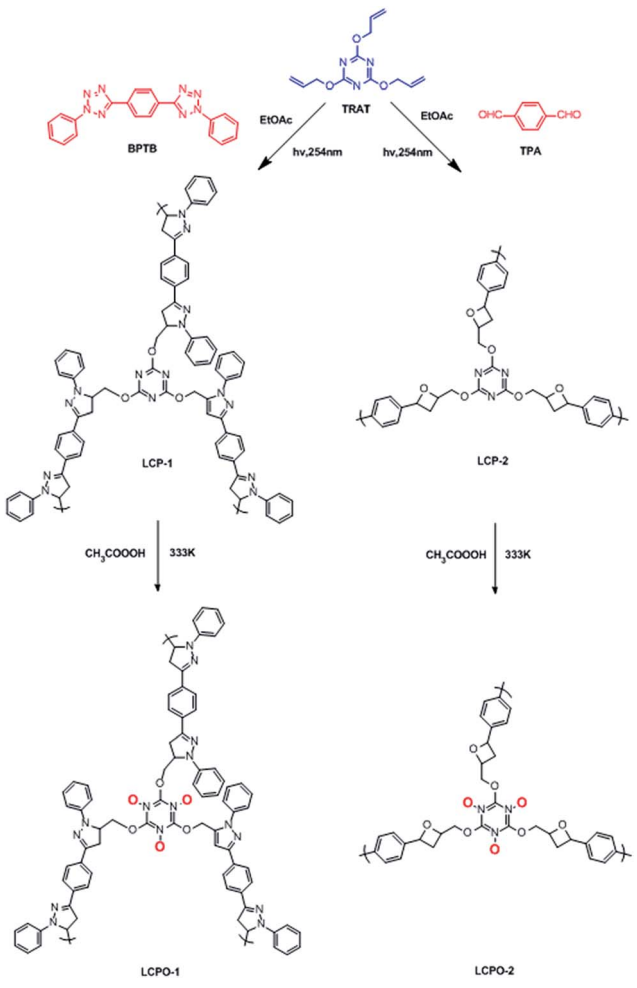

Scheme 1 Synthesis of LCP polymers and schematic diagram of its oxidation LCPO polymers.

Experimental

Materials and measurements

All starting materials were purchased from commercial suppliers and were used without further purification unless otherwise noted.

Thermogravimetric analysis (TGA) was performed using a Netzch Sta 449c thermal analyzer system at A heating rate of 10 °C min^{-1} in air atmosphere. Elemental analyses were measured by Elementar model Vario Micro analyzer. FTIR spectra were measured using a Nicolet Impact 410 Fourier transform infrared spectrometer. The nitrogen adsorption isotherm was measured on an Autosorb iQ2 absorptometer from Quantachrome Instruments. XRD was performed using a Rigaku D/MAX2550 diffractometer with CuKα radiation, 40 kV, 200 mA with a scanning rate of 0.4° min^{-1}. TEM micrographs were recorded using a FEI Tecnai G2F20 s-twin D573 with an acceleration voltage of 300 kV. SEM micrographs were obtained on a JEOL JXA-840 under an accelerating voltage of 15 kV. ^{1}H-NMR spectra were recorded at 400 MHz in DMSO-d_6 as the internal standard with TMS, and solid-state ^{13}C NMR spectra were recorded at 5 KHz. Photoluminescence spectra were recorded on a PerkinElmer LS55 spectrofluorometer. The electronic structures and characteristics for these compounds were explored by density functional theory with Gaussian 09 software at the B3LYP/6-31G(d) level of theory (refer to the ESI for more details†), which has been reported as a good balance between accuracy and computational efficiency.

Synthesis of 1,4-bis(2-phenyl-2*H*-tetrazol-5-yl)benzene (BPTB)

1,4-Bis(2-phenyl-2*H*-tetrazol-5-yl)benzene (BPTB) was synthesized according to a previously described procedure.[49,50] Into a 50 mL Schlenck tube was added 5,5′-(1,4-phenylene)bis(1*H*-tetrazole) (2 mmol, 0.428 g), phenylboronic acid (8 mmol, 0.996 g), Cu_2O (5 mol%, 0.1 mmol, 0.016 g) and DMSO (4 mL). The reaction mixture was stirred under oxygen atmosphere at 100 °C until tetrazole had disappeared, as monitored by TLC. The reaction mixture was then cooled to room temperature and diluted with 100 mL of dichloromethane, washed consecutively with 20 mL of 1 M aqueous HCl and 20 mL of brine (four times). The organic layer was separated and dried over $MgSO_4$, then concentrated under reduced pressure and the pure product was obtained after recrystallization (0.512 g, 1.4 mmol, 70%). ^{1}H NMR ($CDCl_3$, 400 MHz): $\delta = 8.44$ (s, 4H), 8.22–8.24 ppm (d, 4H), 7.59–7.63 ppm (t, 4H), 7.51–7.55 ppm (d, 2H). E. A, calc. for $C_{20}H_{14}N_8$ (%): C, 65.56; H, 3.85. Found: C, 65.00; H, 4.54.

Synthesis of LCP-1

The reaction mechanism for LCP-1 is based on the photoactivatable 1,3-dipolar cycloaddition reaction.[49] Into a 50 mL

a quartz test tube was added 1,4-bis(2-phenyl-2*H*-tetrazol-5-yl) benzene (BPTB) (0.5 mmol, 0.106 g), 2,4,6-tris(allyloxy)-1,3,5-triazine (TRAT) (0.3 mmol, 0.050 g) and ethyl acetate (10 mL). The reaction mixture was stirred under UV irradiation at 254 nm at room temperature for 48 h to afford a yellow precipitate. The resulting yellow solid was stirred in chloroform to remove the unreacted reagents and then washed with various solvents to afford LCP-1 in 85% yield. LCP-1 is insoluble in water and common organic solvents, like dimethyl sulfoxide, methanol, tetrahydrofuran and acetone.

Synthesis of LCP-2

The reaction mechanism for LCP-2 is based on the [2 + 2] Paterno–Büchi reaction.[51] Into a 50 mL a quartz test tube was added terephthalaldehyde (TPA) (0.5 mmol, 0.106 g), 2,4,6-tris(allyloxy)-1,3,5-triazine (TRAT) (0.3 mmol, 0.050 g) and ethyl acetate (10 mL). The reaction mixture was stirred under UV irradiation at 254 nm at room temperature for 48 h to afford a gray precipitate. The resulting gray solid was stirred in chloroform to remove the unreacted reagents and then washed with various solvents to afford LCP-2 in 80% yield. LCP-2 is insoluble in water and common organic solvents, like dimethyl sulfoxide, methanol, tetrahydrofuran and acetone.

Synthesis of LCPO-1 and LCPO-2

LCPO polymers were prepared using a previously described method.[52] 2 g of LCP-1 and 10 mL CH_3COOH and 20 mL of 30% H_2O_2 were mixed. Then the system was sealed to semi-closed, heated to 333 K and kept for 3 hours under stirring condition. After that, the mixture was filtered and the solid was washed with pure water, till the flavor of CH_3COOH could not be smelt. Then the solid was dried at 393 K overnight.

LCPO-2 was also synthesized using the same method with LCP-2 as the reactant.

Photodegradation of methyl orange (MO)

MO solution was prepared in 0.05 mol L^{-1} NaH_2PO_4, 0.05 mol L^{-1} H_3PO_4 and 0.05 mol L^{-1} NaCl buffer solution. A certain amount of catalyst (LCP-1, LCPO-1: 0.100 g, LCP-2 and LCPO-2: 0.100 g) was dispersed in 100 mL of 5 mg L^{-1} MO solution in a Pyrex reactor. After stirring in the dark for 0.5 h, visible light irradiation was provided by a 400 W LED lamp with 420 nm wavelength. During the experiment, the reactor was kept at 298 K by a water bath. An N_2 control experiment was conducted in the same way except N_2 was pumped into the Pyrex reactor from the beginning of the experiment. At suitable time intervals, the mixture was centrifuged and the supernatant was extracted. The concentration of the solution was further analysed by UV at an absorbance wavelength of 465 nm for MO.

Results and discussion

The LCP polymers were characterized by thermogravimetric analysis (TGA), infrared spectroscopy (IR), field-scanning electron microscopy (FE-SEM), transmission electron microscopy (TEM), nitrogen adsorption, cross polarization/magic angle spinning nuclear magnetic resonance (CP/MAS NMR), computational calculation and powder X-ray diffraction (PXRD). TGA results showed that LCP-1 and LCP-2 are stable up to 210 °C and 340 °C in air (Fig. S2†), respectively. The IR spectrum of the LCP polymers exhibits a vibration band characteristic of C=N bonds at 1665 cm^{-1} and 1695 cm^{-1}, respectively. The original vibrational bands separate into double or tripartite peaks suggesting the influence of the N–O bond on the C=N bond of LCP polymers, consistent with a high degree of oxidation (Fig. S3†).[53] CP/MAS NMR spectroscopy gave more information about the structure of the polymers. The signals were assigned to the carbon atoms of the N-heterocyclic rings, triazine rings, oxetane rings and phenyl linkers (Fig. 1c and 2c). For LCP-1, the four intense signals at 168.35, 139.22, 130.98 and 123.01 ppm can be unambiguously assigned to C1/C5, C6/C8, C7/C10 and C9/C11, respectively, in the triazine and benzene rings, while the two relatively weaker signals at 30.08 and 78.51 ppm are attributed to C4 and C2/C3 in the N-heterocyclic rings and $-CH_2$ alkyl groups. For LCP-2, the two intense signals at 172.78 and 128.65 ppm can be unambiguously assigned to C1 and C6/C7, respectively, in the triazine and benzene rings, while the two relatively weaker signals at 33.79 and 82.51 ppm are attributed to C4 and C2/C3/C5 in the oxetane rings and $-CH_2$ alkyl groups.

FE-SEM was used to investigate the morphology of the LCP polymers that were cast from ethyl acetate suspension on Si wafer. The FE-SEM images revealed that the resulting solid was irregular in shape without a well-defined morphology (Fig. 2a). Transmission electron microscopy (TEM) was performed. The TEM images (Fig. 2b) indicated that the texture was largely amorphous. To characterize the nature of the pores, the N_2 sorption of the LCP polymers was measured at 77 K, and exhibited a typical type I isotherm (Fig. 3).

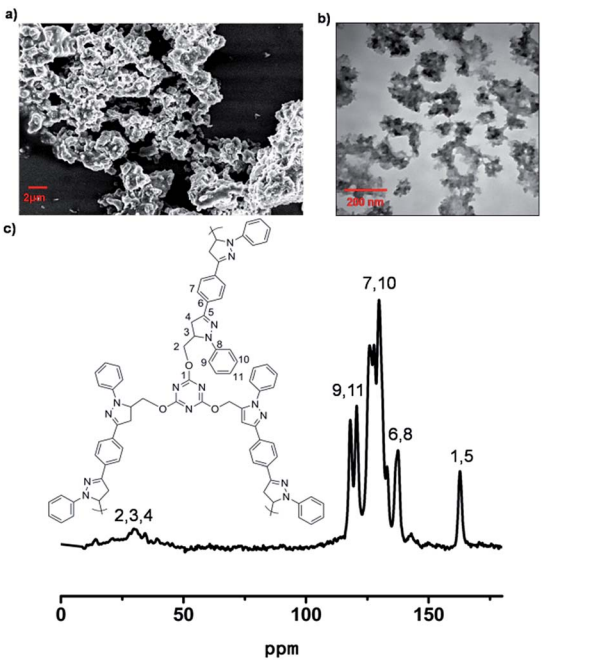

Fig. 1 SEM image (a), TEM image (b), and solid-state ^{13}C NMR spectrum (c) of LCP-1.

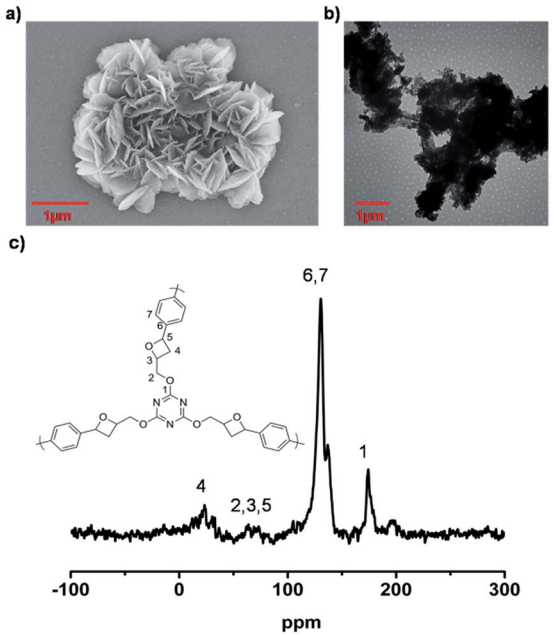

Fig. 2 SEM image (a), TEM image (b), and solid-state ^{13}C NMR spectrum (c) of LCP-2.

In order to confirm the formation of the N–O bond in these polymers, we examined their UV and FL spectra. As displayed in Fig. 4, the introduction of the N–O bond into LCP polymers enhances light harvesting. The possible mechanism is that the π electron conjugation of the whole periodic framework of the LCP polymers is increased by the introduction of the N–O bond into the triazine ring of the LCP polymers.[54,55] Moreover, the FL intensity of the LCP polymers is weaker than that of LCPO polymers, indicating the effective suppressing of the recombination of electron–hole pairs. Therefore, LCPO polymers not only appropriate band gap for the absorption of light to generate charge carriers (electron–hole pairs), but also afford the ability to efficiently separate the carriers, making them suitable photocatalysts.

As shown in Fig. 5, the photocatalytic activities of LCPO-1 and LCPO-2 were evaluated *via* the photodegradation of MO under visible light irradiation. The control experiment was carried out by studying the photolysis of MO for the same duration under visible light irradiation in the absence of a catalyst. It can be seen that MO is stable under visible light irradiation. The different degradation activities for MO treated

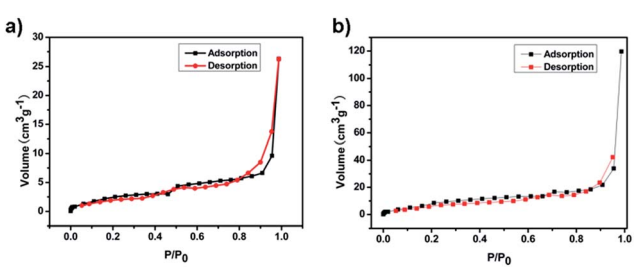

Fig. 3 Nitrogen sorption isotherms of LCP-1 (a) and LCP-2 (b).

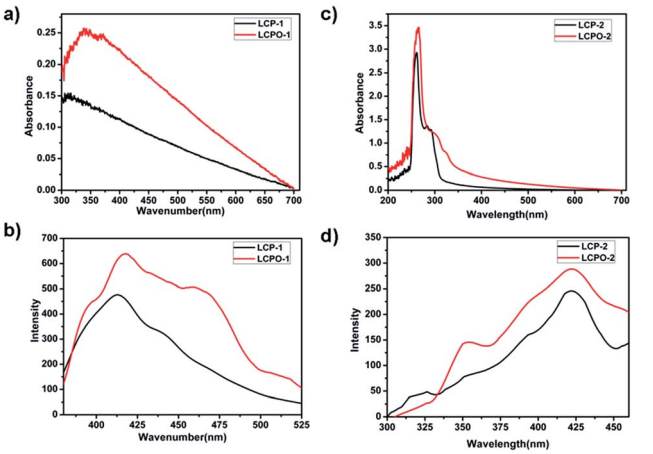

Fig. 4 (a) and (c) UV spectra of LCP and LCPO polymers. (b) and (d) Fluorescence spectra of LCP and LCPO polymers.

in the dark and irradiated with visible light indicate that the degradation of MO on these polymers is indeed driven by visible light. The degradation efficiency (%) can be calculated as efficiency (%) = $(C_0 - C)/C_0 \times 100\%$ (where C_0 is the initial concentration of MO and C is the concentration after photo irradiation).[56] For LCPO-1, when irradiated by visible light, the degradation efficiency of MO was as high as 30%, but the degradation efficiency of MO was as low as 2% treated in the dark in 90 minutes. The photocatalytic activity under light was almost 15 times higher than that in the dark. For LCPO-2, when irradiated by visible light, the degradation efficiency of MO was as high as 24%, but the degradation efficiency of MO was as low as 1% when treated in the dark for 90 minutes. The photocatalytic ability in light was almost 24 times higher than that in dark. Moreover, these results indicate that LCPO-1 has better performance prepared under the same experimental conditions. The XRD patterns of the used LCPO polymers and fresh LCPO polymers were in good agreement, which demonstrates

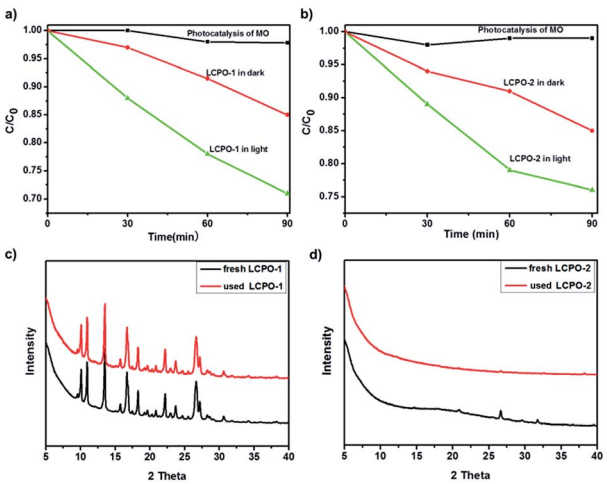

Fig. 5 (a) and (b) Photocatalytic degradation of MO (5 mg L^{-1}) over LCP polymers and LCPO polymers. (c) and (d) PXRD patterns for fresh and used LCPO polymers.

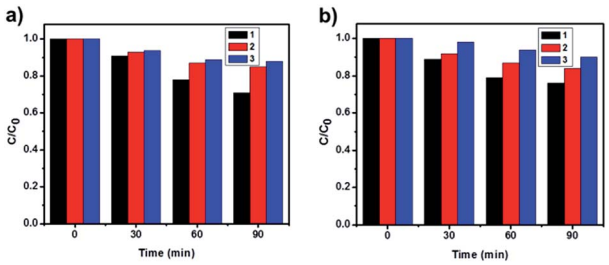

Fig. 6 Cyclic runs of MO degradation by LCPO-1 (a) and LCPO-2 (b).

the stability of the photocatalysts and that they can be reused multiple times.

By virtue of their reusability and stability, heterogeneous catalysts are generally found to be advantageous over homogeneous catalysts. To study the reusability and the stability of the photocatalysts, three successive photocatalytic experiments were carried out by adding used photocatalysts to fresh MO solutions (Fig. 6). No distinct difference in activity was observed, which demonstrates the stability of the catalyst and implies its recyclability. Furthermore, information about the turn over number (TON) and the turn over frequency (TOF) of the catalyst is very important, which tells us about the efficiency of the catalyst.[57] Since the concentration of the reactant (MO) was 1.5×10^{-2} M and the amount of the catalyst was kept at 1 g L^{-1}, for LCPO-1, the calculated TOF of the catalyst for the three cycles were 4.83×10^{16}, 2.50×10^{16} and 2.00×10^{16} molecules per g per s, while for LCPO-2 they were 4.00×10^{16}, 2.40×10^{16} and 1.67×10^{16} molecules per g per s. Therefore, LCPO-1 and LCPO-2 can be used as high-performance and stable visible-light photocatalysts and they have potential applications in environmental protection.

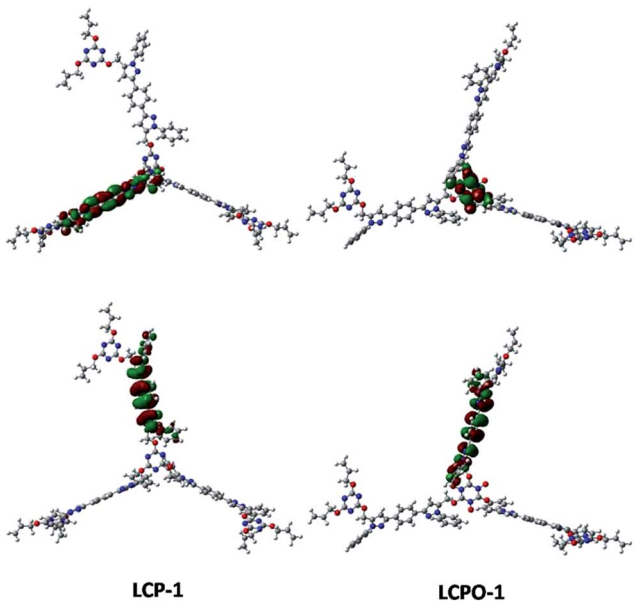

Fig. 7 LUMO (above) and HOMO (below) of LCP-1 (left) and LCPO-1 (right) samples. Carbon, nitrogen and oxygen in the structural models are shown as gray, blue and red spheres, respectively.

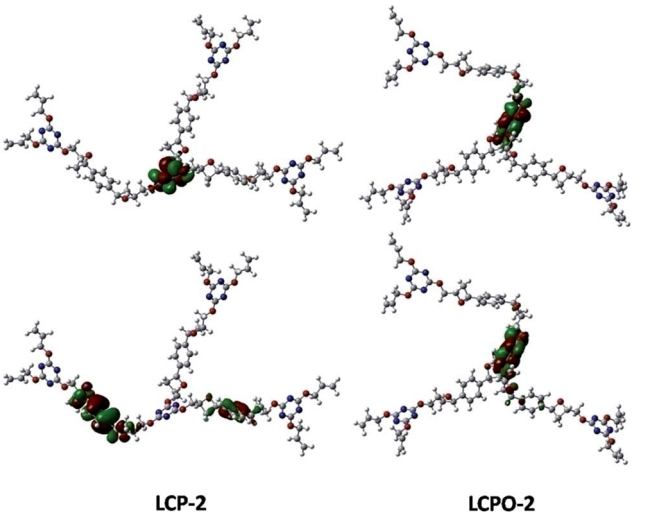

Fig. 8 LUMO (above) and HOMO (below) of LCP-2 (left) and LCPO-2 (right) samples. Carbon, nitrogen and oxygen in the structural models are shown as gray, blue and red spheres, respectively.

To improve our understanding of the electronic structure change, theoretical calculations have been carried out. The HOMO and LUMO analyses reveal that the energy of the LUMO is −1.01 eV in LCP-1 and −2.18 eV in LCPO-1, while the energy of the LUMO is −0.39 eV in LCP-2 and −1.99 eV in LCPO-2. In addition, from the HOMO and LUMO positions of the LCP polymers and the LCPO polymers (Fig. 7 and 8), it is obvious that the HOMO does not change, both in LCP-1/LCPO-1 and LCP-2/LCPO-2, while the LUMO has changed. Briefly, compared to LCP polymers, LCPO polymers have a lower HOMO–LUMO band, thus the activity goes up under visible light irradiation, meaning that the electrons are excited from the HOMO to the LUMO of the photocatalyst easier. Meanwhile, the N–O bond interacts strongly with polar compounds owing to the strong polar bond ($^{+}$N–O^{-}),[58] which endows the LCPO polymers with an adsorption-photocatalysis synergistic effect, and leads to the effective degradation of the pollutant. This result indicates that the introduced N–O bond plays an important role in improving the photocatalytic activity. The photocatalytic efficiencies (LCPO-1 > LCPO-2) may be owing to the energy gap between the LUMO and HOMO.[59] Such differences may result in the faster generation speed of photo-generated holes and electrons in LCPO-1 and the faster decomposition of MO initiated by LCPO-1.

Conclusions

In conclusion, we have synthesized two new cross-linked polymers (LCP-1 and LCP-2) based on light-induced click cross-coupling reaction strategy. The polymeric aromatic N-oxides (LCPO-1 and LCPO-2) as organic photocatalysts showed great potential in the photodegradation of MO in solution. The strong polar N–O bond enhances the oxidation ability of the photo-induced hole, making an excellent synergistic effect with the unique electronic structure of the parent polymers. This work

opens a new avenue to develop efficient heterogeneous catalytic systems to solve problems of environmental pollution and energy shortage.

Acknowledgements

This work was supported by the National Natural Science Foundation of China (Project No. 21601177).

Notes and references

1 J. J. Wang and R. B. Bai, *Water Res.*, 2016, **101**, 103–113.
2 V. K. Gupta and Suhas, *J. Environ. Manage.*, 2009, **90**, 2313–2342.
3 G. McMullan, C. Meehan, A. Conneely and W. F. Smyth, *Appl. Microbiol. Biotechnol.*, 2001, **56**, 81–87.
4 C. I. Pearcea, J. R. Lloyd and J. T. Guthrie, *Dyes Pigm.*, 2003, **58**, 179–196.
5 A. T. Chow, D. M. Leech, T. H. Boyer and P. C. Singer, *Environ. Sci. Technol.*, 2008, **42**, 5586–5593.
6 M. H. Lee and J. Hur, *Clean: Soil, Air, Water*, 2014, **42**, 552–560.
7 Q. Y. Wu, C. Li, W. L. Wang, T. He, H. Y. Hu, Y. Du and T. Wang, *J. Environ. Sci.*, 2016, **43**, 118–127.
8 J. J. Wang and R. B. Bai, *Water Res.*, 2016, **101**, 103–113.
9 A. Kudo and Y. Miseki, *Chem. Soc. Rev.*, 2009, **38**, 253–278.
10 S. Sato, T. Morikawa, S. Saeki, T. Kajino and T. Motohiro, *Angew. Chem., Int. Ed.*, 2010, **49**, 5101–5105.
11 Y. Liu, B. Huang, Y. Dai, X. Zhang, X. Qin, M. Jiang and M. Whangbo, *Catal. Commun.*, 2009, **11**, 210–213.
12 X. Li, L. Wang, G. J. Chen, D. M. Haddletonc and H. Chen, *Chem. Commun.*, 2014, **50**, 6506–6508.
13 T. P. Yoon, M. A. Ischay and J. Du, *Nat. Chem.*, 2010, **2**, 527–532.
14 H. Tong, S. Ouyang, Y. Bi, N. Umezawa, M. Oshikiri and J. Yeet, *Adv. Mater.*, 2012, **4**, 229–251.
15 X. Chen, S. Shen, L. Guo and S. Mao, *Chem. Rev.*, 2010, **110**, 6503–6570.
16 C. Chen, W. Ma and J. Zhao, *Chem. Soc. Rev.*, 2010, **39**, 4206–4219.
17 X. B. Chen and A. Selloni, *Chem. Rev.*, 2014, **114**, 9281–9282.
18 G. Liu, H. Yang, J. Pan, Y. Yang, G. Lu and H. Cheng, *Chem. Rev.*, 2014, **114**, 9559–9612.
19 M. Kapilashrami, Y. Zhang, Y. Liu, A. Hagfeldt and J. Guo, *Chem. Rev.*, 2014, **114**, 9662–9707.
20 Y. Chen, H. J. Cui, J. Q. Zhang, K. Zhao, D. F. Ding, J. Guo, L. S. Li, Z. Y. Tian and Z. Y. Tang, *RSC Adv.*, 2015, **5**, 92573–92576.
21 T. Ratvijitvech, R. Dawson, A. Laybourn, Y. Z. Khimyak, D. J. Adams and A. I. Cooper, *Polymer*, 2014, **55**, 321–325.
22 A. I. Cooper, *Adv. Mater.*, 2009, **21**, 1291–1295.
23 C. A. Wang, Y. F. Han, Y. W. Li, K. Nie, X. L. Cheng and J. P. Zhang, *RSC Adv.*, 2016, **6**, 34866–34871.
24 D. X. Wang, W. Y. Yang, S. Y. Feng and H. Z. Liu, *Polym. Chem.*, 2014, **5**, 3634–3642.
25 L. J. Feng, Q. Chen, J. H. Zhu, D. P. Liu, Y. C. Zhao and B. H. Han, *Polym. Chem.*, 2014, **5**, 3081–3088.
26 X. W. Yang, X. D. Zhuang, Y. J. Huang, J. Z. Jiang, H. Tian, D. Q. Wu, F. Zhang, Y. Y. Mai and X. L. Feng, *Polym. Chem.*, 2015, **6**, 1088–1095.
27 X. D. Li, S. Q. Feng, F. Guo, X. Y. Liu, J. X. Yu and Z. W. Hou, *RSC Adv.*, 2016, **6**, 21517–21525.
28 D. Y. Chen, S. Gu, Y. Fu, Y. L. Zhu, C. Liu, G. H. Li, G. P. Yu and C. Y. Pan, *Polym. Chem.*, 2016, **7**, 3416–3422.
29 T. Fei, K. Jiang, S. Liu and T. Zhang, *RSC Adv.*, 2014, **4**, 21429–21434.
30 X. D. Li, J. H. Guo, H. Zhang, X. L. Cheng and X. Y. Liu, *RSC Adv.*, 2014, **4**, 24526–24532.
31 S. Xu, K. Song, T. Li and B. Tan, *J. Mater. Chem. A*, 2015, **3**, 1272–1278.
32 W. J. Zhang, P. P. Jiang, Y. Wang, J. Zhang, Y. X. Gao and P. B. Zhang, *RSC Adv.*, 2014, **4**, 51544–51547.
33 R. Dawson, D. J. Adams and A. I. Cooper, *Chem. Sci.*, 2011, **2**, 1173–1177.
34 C. G. Bezzu, M. Carta, A. Tonkins, J. C. Jansen, P. Bernardo, F. Bazzarelli and N. B. McKeown, *Adv. Mater.*, 2012, **24**, 5930–5933.
35 Y. H. Xu, S. B. Jin, H. Xu, A. Nagai and D. L. Jiang, *Chem. Soc. Rev.*, 2013, **42**, 8012–8031.
36 Y. Q. Yang, Q. Zhang, J. F. Zheng and S. B. Zhang, *Polymer*, 2013, **54**, 3254–3260.
37 S. Yuan, S. Kirklin, B. Dorney, D. J. Liu and L. Yu, *Macromolecules*, 2009, **42**, 1554–1559.
38 Z. G. Xie, C. Wang, K. E. deKrafft and W. B. Lin, *J. Am. Chem. Soc.*, 2011, **133**, 2056–2059.
39 J. X. Jiang, Y. Li, X. Wu, J. Xiao, D. J. Adams and A. I. Cooper, *Macromolecules*, 2013, **46**, 8779–8783.
40 N. Kang, J. H. Park, K. C. Ko, J. Chun, E. Kim, H. W. Shin, S. M. Lee, H. J. Kim, T. K. Ahn, J. Y. Lee and S. U. Son, *Angew. Chem., Int. Ed.*, 2013, **52**, 6228–6232.
41 L. Pan, M. Y. Xu, L. J. Feng, Q. Chen, Y. J. He and B. H. Han, *Polym. Chem.*, 2016, **7**, 2299–2307.
42 Q. Sun, Z. F. Dai, X. J. Meng and F. S. Xiao, *Chem. Soc. Rev.*, 2015, **44**, 6018–6034.
43 L. M. Campos, K. L. Killops, R. Sakai, J. M. J. Paulusse, D. Damiron, E. Drockenmuller, B. W. Messmore and C. J. Hawker, *Macromolecules*, 2008, **41**, 7063–7070.
44 C. E. Hoyle, A. B. Lowe and C. N. Bowman, *Chem. Soc. Rev.*, 2010, **39**, 1355–1387.
45 B. J. Adzima, Y. Tao, C. J. Kloxin, C. A. DeForest, K. S. Anseth and C. N. Bowman, *Nat. Chem.*, 2011, **3**, 256–259.
46 P. Xiao, F. Dumur, M. A. Tehfe, B. Graff, D. Gigmes, J. P. Fouassier and J. Lalevéea, *Polymer*, 2013, **54**, 3458–3466.
47 S. Telitel, F. Dumur, D. Gigmes, B. Graff, J. P. Fouassier and J. Lalevée, *Polymer*, 2013, **54**, 2857–2864.
48 W. L. Li, Z. G. Xie and X. B. Jing, *Catal. Commun.*, 2011, **16**, 94–97.
49 Y. X. Li, W. Zhang, Z. Y. Sun, T. T. Sun, Z. G. Xie, Y. B. Huang and X. B. Jing, *Eur. Polym. J.*, 2015, **63**, 149–155.
50 Y. X. Li, Z. Y. Sun, T. T. Sun, L. Chen, Z. G. Xie, Y. B. Huang and X. B. Jing, *RSC Adv.*, 2013, **3**, 21302–21305.
51 M. Conradi and T. Junkers, *Macromolecules*, 2011, **44**, 7969–7976.
52 E. Ochiai, *J. Org. Chem.*, 1953, **18**, 534–551.

53 J. C. Yang, S. Chu, Y. Guo, L. L. Luo, F. Kong, Y. Wang and Z. G. Zou, *Chem. Commun.*, 2012, **48**, 3533–3535.
54 C. C. Wang, Y. Guo, Y. Yang, S. Chu, C. K. Zhou, Y. Wang and Z. G. Zou, *ACS Appl. Mater. Interfaces*, 2014, **6**, 4321–4328.
55 S. Chu, Y. Wang, Y. Guo, P. Zhou, H. Yu, L. L. Luo, F. Kongab and Z. G. Zou, *J. Mater. Chem.*, 2012, **22**, 15519–15521.
56 S. C. Yan, Z. S. Li and Z. G. Zou, *Langmuir*, 2010, **26**, 3894–3901.
57 S. Gazi and R. Ananthakrishnan, *Appl. Catal., B*, 2011, **105**, 317–325.
58 M. H. Abraham, L. Honcharova, S. A. Rocco, W. E. Acree and K. M. DeFina, *New J. Chem.*, 2011, **35**, 930–936.
59 D. X. Li, C. Y. Ni, M. M. Chen, M. Dai, W. H. Zhang, W. Y. Yan, H. X. Qi, Z. G. Ren and J. P. Lang, *CrystEngComm*, 2014, **16**, 2158–2167.